BTDF MEASUREMENTS AND RAY-TRACING SIMULATIONS COMPARISONS FOR PRISMATIC GLAZING

Marilyne Andersen, Solar Energy and Building Physics Laboratory, EPFL, Switzerland, *presents a detailed validation approach for bi-directional properties of complex fenestration systems*

Introduction

Evaluation of solar heat gain and daylight distribution through complex window and shading systems requires the determination of the Bi-directional Transmission Distribution Function (BTDF). In this paper, measurements and ray-tracing-based calculations are compared for the specific case of prismatic daylight-redirecting panels. The latter have been chosen as a validation example because they consist of a material of well-known refraction coefficients, thus easily handled by the software applying Snell-Descartes' law, whereas at the same time they present complex transmission features because of the multiple inside reflections and interactions between the gratings.

Measurements were performed in a photogoniometer equipped with a digital-imaging detection system (Andersen ***et al.,*** 2001), developed at the Swiss Federal Institute of Technology (EPFL), which allows to considerably reduce time-consumption when characterizing a fenestration system (2 to 4 minutes per incident direction) and to get a continuous knowledge of the whole transmission space, averaged into zones, instead of discrete transmission assessments that need to be interpolated. A virtual copy of the photogoniometer was constructed with the commercial forward ray-tracing software TRACEPRO® (v. 2.3 & 2.4, Lambda Research Corporation) based on Monte-Carlo calculations. For the first time, an attempt is made to validate detailed bi-directional properties for a complex system. The results generally agree under a range of input and output angles to a degree adequate for evaluation of glazing systems. Calculations were also performed using a more realistic model of the source and ideal model of the detector. Deviations from the photogoniometer model were small and the results were similar in form. Despite the lack of an absolute measurement standard, the good agreement in results promotes confidence in both the photogoniometer and in the calculation method.

BTDF characterization conditions

The incident source that has been used for BTDF characterization consists of a HMI 2.5 kW discharge lamp with a Fresnel lens. Its spectrum has been measured and has been approximated by a discrete set of 34 wavelengths for the simulation model; the virtual incident beam has been defined as of same angular (lambertian) spread as the real one, and positioned in order to simulate the same incident directions as the ones analyzed (in fact placed against the outside sample interface and emitting rays at varying direction vectors, depending on the incident direction considered, to have a unique geometric situation and avoid a weighing of the incoming light flux). The rays are emitted from a circular grid sending about 200'000 rays (~6'000 rays for each wavelength). The flux threshold is set to 0.05. It has been checked that a larger number of rays (e.g. 15'000 per wavelength) or a lower cut-off value (e.g. 0.001) do not significantly affect the results, inducing differences lower than 1% whereas considerably increasing time-consumption. A set of 6 detection planes of same geometry as the one used as a projection screen in the measurement facility and separated into the same pattern of discretization zones (solid angles around outgoing directions) has been built in TRACEPRO®, together with a sample of same geometric and physical (acrylic) properties as the ones measured, and exposing a sample area that fits the illuminated surface during experimental characterization.

Of course, the virtual BTDF assessment will still be a theoretical model of what the experimental set-up was expected to be, as the sample is considered of perfect shape and condition, and of transmission properties strictly defined by Snell's refraction laws.

Ray-tracing output

For each prismatic panel, five representative incidences have been selected, for varying altitudes and azimuths: the chosen angular couples (q_1, f_1) are: for the symmetric panel (flat face on incident side), (40°, 90°), (60°, 90°), (24°, 30°), (40°, 45°) and (60°, 75°); for the asymmetric panel, (20°, 0°) and (40°, 90°) for the flat face on incident side, (0°, 0°), (10°, 90°) and (20°, 270°) for the gratings on the incident side.

As we are here interested in daylighting features, the quantity that is detected is the total photometric flux [lumen] received by each discretization surface, easily convertible into the associated BTDF value through equation (1), where.

$$BTDF(\theta_1,\phi_1,\theta_2,\phi_2)\left[sr^{-1}\right] = \frac{L_2}{E_1} = \frac{\Phi_2}{\Omega_2 \cdot A\cos\theta_2} \cdot \frac{A}{\Phi_1} = \frac{\Phi_{2,meas}[\%]}{\Delta\theta_2 \cdot \Delta\phi_2 \cdot \sin\theta_2 \cdot \cos\theta_2}$$

where (θ_1, φ_1) and (θ_2, φ_2) are the polar co-ordinates of, respectively, the incoming and emerging (transmitted) light flux [°], A is the illuminated area of the sample [m²]

and $E_1(q_1)$ its illuminance [lx] (due to the incoming light flux), and L_2 [cd m^{-2}] is the luminance of the emerging (transmitted) light flux F_2. (Dq_2, Df_2) is the angular output resolution (determining the discretization zones)

It can be noted that detecting the transmitted light directly on a virtual panel (100% absorbing to avoid inter-reflections) instead of the physical diffusing screen allows an accurate estimation of the measurement error induced by the camera's calibration procedures (spectral, photometric, geometric, additional corrections).

The obtained simulation model is shown on Fig. 1A for the symmetric prism. Fig. 1B gives an example of ray-trace plot (the rays appearing towards the left are reflected, thus not detected). On this figure, one can observe two main peaks in transmission, caused by the prismatic structure (gratings), with a spread of the outgoing rays induced mainly by the dependence of the acrylic refractive indices with the wavelength.

Note that both experimental and simulated BTDF values are here assessed inside a certain angular area around the associated couples (θ_2, φ_2), and depend on the output resolution ($\Delta\theta_2$, $\Delta\varphi_2$), - they represent average BTDF values inside these areas -, providing a continuous transmitted light distribution, unlike point-per-point BTDF measurements.

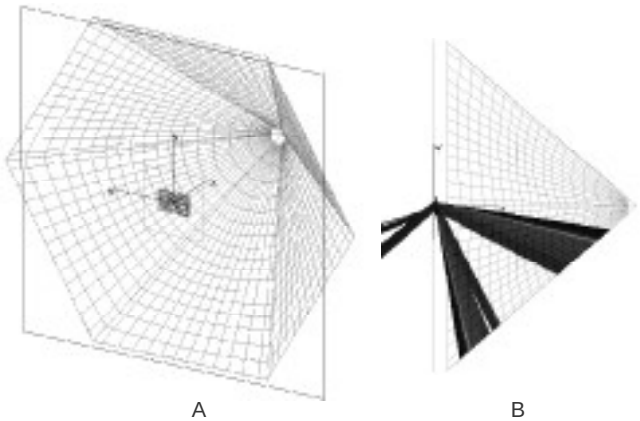

A B

Fig. 1. (A) Simulation model, angular zones ($\Delta\theta_2$, $\Delta\varphi_2$)=(5°, 5°). (B) Ray-tracing plots, incidence (θ_1, φ_1)=(40°, 90°).

Results comparison

The most synthetic and intuitive approach of representing BTDF data graphically is to create 3D plots in spherical coordinates, called photometric solids and described in (Andersen, 2002). However, as the transmission features for the two analyzed samples happen to be very sharp, conventional section views along most relevant azimuths f_2 (i.e. where BTDFs are non-zero) and for varying altitudes q_2 are preferred, to reveal the discrepancies between measurement and simulation more accurately than by showing global views, where small differences might be difficult to notice.

Four incidences out of the 10 directions investigated are shown in Figs. 2 and 3, where one can observe either one or two BTDF peaks for each incident direction; these graphs as well as the other comparison curves reveal a very good agreement between the two methods, even though the transmission features are extremely sharp (high gradients indeed increase the risk of having significant differences), with especially low BTDF discrepancies and a very similar qualitative light behaviour, the peaks being every time along exactly the same directions.

The error bars given on all the figures for the experimental and computational BTDF data are 13% and 10%, respectively, in relative terms. The uncertainties due to the CCD camera calibration procedures and other corrections have been investigated thoroughly in (Andersen ***et al.***, 2000); to these uncertainties have been added the discrepancies connected to the spatial adjustment of the facility components, estimated by modelling slight variations (±0.5°, ±2 mm) in the incident direction or detection screen and observing the effect on the final results. This has lead to a global error of 13% for the measurements. The 10% uncertainty for the model includes the very small variations of results with the threshold, the spectrum discretization and the number of emitted rays (~1% for each parameter). The model uncertainty also includes the impact of the simplification hypotheses in the prism modelling, which was assessed by changing slightly some simulation parameters (rounded edges 0.25 mm off the theoretical summits, 1% variations in the refraction indices, 2% diffuse component added on prism surface for wearing, etc.).

Considering the high sensitivity of the results to the exact outgoing rays direction and weight, the peak values being very narrow, the comparison of BTDF data obtained for the two prismatic elements and the different incident directions given on Figs. 2 and 3 shows close behaviour. This indicates a positive reciprocal validation on one hand of the detection technique together with the calibration and correction procedures accuracy, and on the other hand of the reliability and applicability of ray-tracing calculations for complex glazing assessment.

On Figs. 2 and 3 a third curve has been added; providing BTDF values from the simulation model of a so-called ideal set-up, based on the following hypotheses: a parameterised sun as the incident source, i.e. a beam of spectrum given by the sun's radiation properties, and of almost perfect collimation (half-angle 0.25°), and a virtual hemispherical detector, discretized according to the adequate resolution ($\Delta\theta_2$, $\Delta\varphi_2$) – only partly for a more convenient assignment of zones – and of optimal radius, shown on Fig. 4 with a ray-tracing plot under incidence (10°, 90°) for the asymmetric panel (reflected rays on the left). Indeed, even though a flat projection screen is preferable with an experimental light distribution assessment as it avoids any risk of inter-reflection, a hemisphere appears to be a more ideal detection system, the light being then collected at a constant distance from the sample, and on a surface normal to the rays.

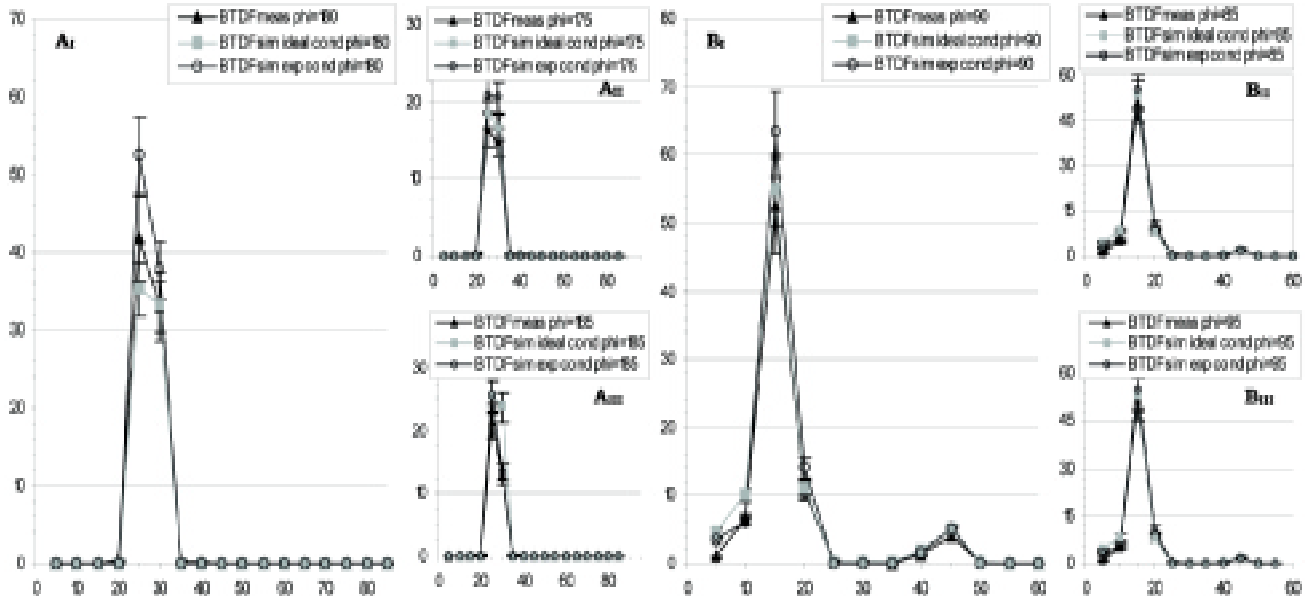

Fig. 2. BTDF [sr^{-1}] vs. θ_2 [°] along φ_2 planes: comparison of measurements (BTDFmeas) and calculations with experimental (BTDFsim exp) and ideal (BTDFsim ideal) conditions. (A) Symmetric panel, flat glass on incident side, incidence (40°, 45°). (B) Asymmetric panel, gratings on incident side, incidence (10°, 90°).

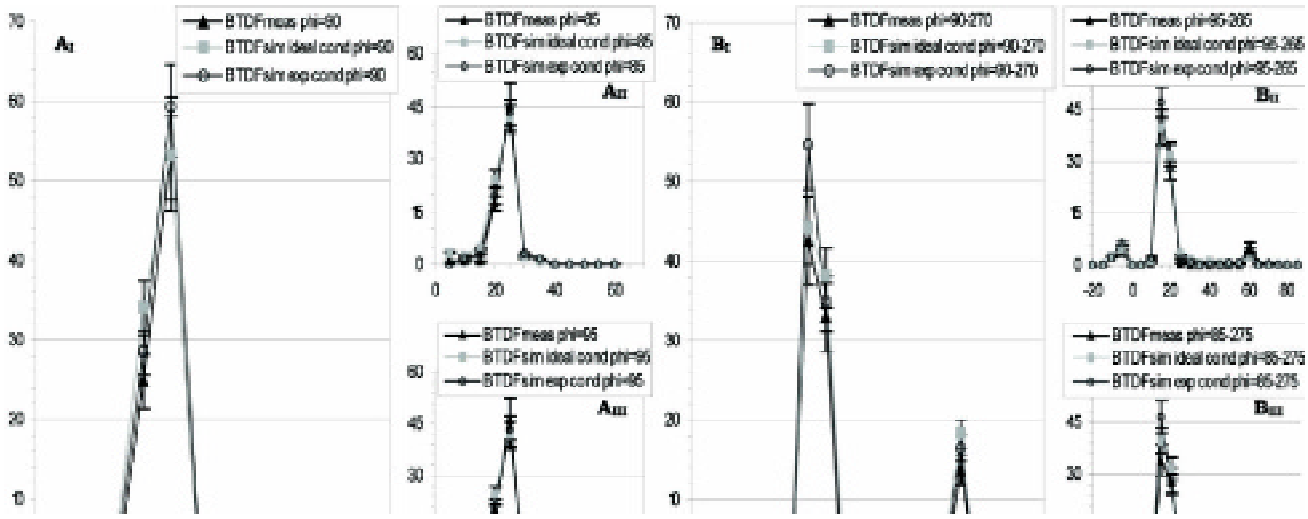

Fig. 3. BTDF [sr^{-1}] vs. θ_2 [°] along φ_2 planes: comparison of measurements (BTDFmeas) and calculations with experimental (BTDFsim exp) and ideal (BTDFsim ideal) conditions. (A) Asymmetric panel, gratings on incident side, incidence (0°, 0°). (B) Asymmetric panel, flat face on incident side, incidence (40°, 90°).

On this figure, one clearly observes the spread of transmitted rays caused by the dependence of the refractive index on the wavelength value. All the same, as shown on Figs. 2 and 3, light is still transmitted along sharp peaks, not observable on Fig. 4, firstly because the human eye sensitivity is taken into account for photometric flux estimations, with a greatly varying importance assigned to rays of different wavelengths, and secondly because ray-tracing plots cannot provide a quantitative information on the weight of each ray.

The discrepancies observed when comparing measurement conditions with ideal simulation results on the curves in Figs. 2 and 3 remain very low, and show coherent behaviours (peaks along the same directions, similar BTDF values). The differences are generally even lower than for the experimental conditions model, which tends to prove that the new parameters (source spectrum, beam spread, detector) tend to compensate each other's effects, and that the light distribution will be assessed likewise, whether using the experimental facility or a more ideal set-up.

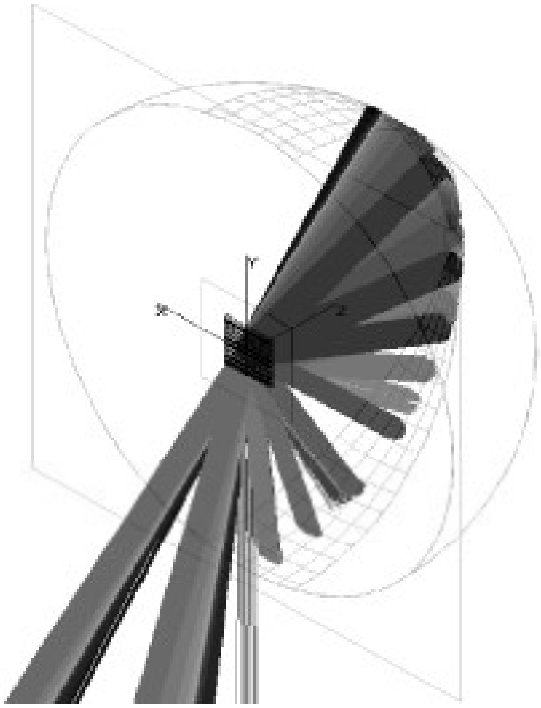

Fig. 4: Ideal simulation model hemispherical detector of adjusted radius. Asymetric panel, Incidence (10°,90°)

Conclusion

Lacking absolute standards for measurement of BTDF on full-scale systems, validation must be approached in a roundabout manner. The Monte Carlo calculation is based on first-principles and applied with algorithms that have been widely tested on a variety of optical systems. The inputs are either easily-specified geometrical descriptions or result from standardized optical measurements. Thus, there is every reason to believe that the results will be accurate. Conversely, the calculations agree with the measurements from a photogoniometer of carefully executed construction, that has been validated on simple systems of well-known properties.

The computational method also proved to be a valuable tool for variation of parameters. First, agreement was established using the closest possible virtual copy of the physical photogoniometer. Then, more realistic parameters were set to test effects of various compromises made in the construction of the light source, detector screen, camera and other components of the real photogoniometer. The results showed that the assumptions made in the construction of the instrument were reasonable and easily extended by calculation to even more realistic conditions.

The importance of these results goes beyond validation of the specific glazing and instrument of this study. We deliberately chose a glazing system that would be difficult to reproduce in some aspects. It is plausible, therefore, that this method will be quite general and could reduce the burden of difficult and time-consuming measurements on complex systems. Also, when further confidence in this approach has been established, validation will be facilitated among the disparate and incomparable measurement systems worldwide.

References

Andersen, M., Michel, L., Roecker, C. and Scartezzini J.-L. (2001), Experimental assessment of bi-directional transmission distribution functions using digital imaging techniques, ***Energy and Buildings* 33** (5), 417-431.

Andersen M. (2002), Light distribution though advanced fenestration systems. ***Building Research and Information* 30** (4), 264-281.

Andersen, M., Scartezzini J.-L., Michel, L. and Roecker, C. (2000), Bi-directional Photogoniometer for the Assessment of the Luminous Properties of Fenestration Systems. CTI Project No. 3661.2, LESO-PB/EPFL (Ed), Lausanne.